Solving critical point conditions for the Hamming and taxicab distances to solution sets of polynomial equations

Danielle A. Brake*, Noah S. Daleo†, Jonathan D. Hauenstein‡ and Samantha N. Sherman‡
*Department of Mathematics
University of Wisconsin–Eau Claire, Eau Claire, WI, 54701
brakeda@uwec.edu
†Department of Mathematics
Worcester State University, Worcester, MA, 01602
ndaleo@worcester.edu
‡Department of Applied and Computational Mathematics and Statistics
University of Notre Dame, Notre Dame, IN 46656
{hauenstein,ssherma1}@nd.edu

***Abstract*—Minimizing the Euclidean distance (ℓ_2-norm) from a given point to the solution set of a given system of polynomial equations can be accomplished via critical point techniques. This article extends critical point techniques to minimization with respect to Hamming distance (ℓ_0-"norm") and taxicab distance (ℓ_1-norm). Numerical algebraic geometric techniques are derived for computing a finite set of real points satisfying the polynomial equations which contains a global minimizer. Several examples are used to demonstrate the new techniques.**

***Keywords*-Numerical algebraic geometry; real solutions; Hamming distance; taxicab distance; critical points.**

I. Introduction

Two common non-smooth objective functions arising in applications are the Hamming distance (ℓ_0-"norm") [1] and the taxicab distance (ℓ_1-norm). For example, one problem in compressed sensing [2], [3] is to obtain the sparsest vector which satisfies a linear system. That is, given $A \in \mathbb{R}^{n\times N}$ and $y \in \mathbb{R}^n$, solve

$$\min\{\|x\|_0 \,:\, Ax = y\} \tag{1}$$

where $x \in \mathbb{R}^N$ and $\|x\|_0 = \#\{j \,:\, x_j \neq 0\}$. A common technique for trying to solve (1) is to replace the Hamming distance $\|x\|_0$ with the taxicab distance $\|x\|_1 = \sum_i |x_i|$, namely by solving the convex optimization problem

$$\min\{\|x\|_1 \,:\, Ax = y\}. \tag{2}$$

Some additional applications include error correction [4], facial recognition [5], and magnetic resonance imaging [6].

Rather than consider solutions to linear equations as in (1) and (2), we consider constraint sets which are the solution set to a system of polynomial equations having real coefficients. That is, for a real polynomial system $g : \mathbb{R}^N \to \mathbb{R}^n$, let

$$\mathcal{V}_{\mathbb{C}}(g) = \{x \in \mathbb{C}^N \,:\, g(x) = 0\} \text{ and } \mathcal{V}_{\mathbb{R}}(g) = \mathcal{V}_{\mathbb{C}}(g) \cap \mathbb{R}^N,$$

commonly called the complex and real variety of g, respectively. We aim to solve

$$\min\{\|x\|_0 \,:\, x \in \mathcal{V}_{\mathbb{R}}(g)\} \tag{3}$$

and

$$\min\{\|x\|_1 \,:\, x \in \mathcal{V}_{\mathbb{R}}(g)\}. \tag{4}$$

Since $\mathcal{V}_{\mathbb{R}}(g)$ need not be convex, (4) need not be a convex program in contrast to the convex program (2).

An early method for solving the sparse-solution problem was the greedy algorithm in compressive sensing [7]. A subsequent method is *basis pursuit* stemming from [8], where one represents a function, or signal, in terms of an existing dictionary of basis functions. More recent methods have included nonlinear basis pursuit (NBP), where the problem has arisen as nonlinear compressive sensing [9], which is an iterative method using monomial representation to solve a convex version of (4).

A problem related to (3) and (4) is the Euclidean distance (ℓ_2-norm) minimization problem

$$\min\{\|x\|_2^2 \,:\, x \in \mathcal{V}_{\mathbb{R}}(g)\} \tag{5}$$

where $\|x\|_2^2 = \sum_i x_i^2$. This problem has been studied extensively in computational algebraic geometry via critical point conditions. For example, in addition to containing a global minimizer of (5), Seidenberg showed in [10] that the set of critical points of (5) also contains a point on each connected component of $\mathcal{V}_{\mathbb{R}}(g)$. Modifications of this method which compute a finite subset of critical points containing a global minimizer as well as a point on each connected component were developed in [11], [12] with the term *Euclidean distance degree* coined in [13], [14]. Model selection [15] is one of many applications of solving (5). For more details on basic algebraic geometry, see [16], [17].

Following a similar strategy, this paper develops critical point systems consisting of polynomial equations for (3)

and (4). Then, under genericity assumptions, we construct a homotopy-based method to compute a finite set of critical points which contains a global minimizer. Hence, a global minimizer can be obtained via a post-processing search of the finite set of critical points.

The rest of the paper is organized as follows. Section II derives polynomial necessary conditions for (3) and (4). Section III describes a homotopy-based approach for computing a finite set of solutions satisfying these necessary conditions. Section IV provides local homotopy methods for obtaining a critical point starting from a given point. We conclude with additional examples in Section V.

II. Necessary conditions

For a real polynomial system $g : \mathbb{R}^N \to \mathbb{R}^n$, the following reviews necessary conditions for (5) and then extends to necessary conditions for (3) and (4).

A. Minimizing $\|x\|_2$

For $a \in \mathbb{R}^N$, the following proposition provides Fritz John [18] necessary conditions for solving

$$\min\{\|x-a\|_2^2 \,:\, x \in \mathcal{V}_{\mathbb{R}}(g)\}. \tag{6}$$

Note that it must be the case that either $\mathcal{V}_{\mathbb{R}}(g) = \emptyset$ or (6) has a global minimum. Let $\mathbb{P}^n$ denote n-dimensional projective space.

Proposition II.1. *If $x^* \in \mathcal{V}_{\mathbb{R}}(g)$ solves* (6)*, then there exists $\lambda^* \in \mathbb{P}^n$ such that $G(x^*, \lambda^*) = 0$ where*

$$G(x,\lambda) = \begin{bmatrix} g(x) \\ \lambda_0(x-a) + \sum_{i=1}^n \lambda_i \nabla g_i(x) \end{bmatrix} \tag{7}$$

and $\nabla g_i(x)$ is the gradient of g_i evaluated at x.

The system G in (7) is the *critical point system* for (6) and the set of *critical points* of (6) is the set of points x such that there exists $\lambda \in \mathbb{P}^n$ with $G(x,\lambda) = 0$.

Example II.2. For $g(x) = x_1^2 + x_2^2 - 1$ and $a = (-0.6, 0.45)$, the critical point system

$$G(x,\lambda) = \begin{bmatrix} x_1^2 + x_2^2 - 1 \\ \lambda_0 \begin{bmatrix} x_1 + 0.6 \\ x_2 - 0.45 \end{bmatrix} + \lambda_1 \begin{bmatrix} 2x_1 \\ 2x_2 \end{bmatrix} \end{bmatrix}$$

yields two critical points, namely $p_1 = (-0.8, 0.6)$ and $p_2 = (0.8, -0.6)$ which are shown in Figure 1. It is easy to verify that p_1 and p_2 are the global minimizer and maximizer, respectively, for (6).

B. Minimizing $\|x\|_0$

For $a \in \mathbb{R}^N$, we aim to derive necessary conditions for

$$\min\{\|x-a\|_0 \,:\, x \in \mathcal{V}_{\mathbb{R}}(g)\} \tag{8}$$

via a polynomial system. Two difficulties are that the map $x \mapsto \|x-a\|_0$ is not continuous and thus not differentiable, and there need not be isolated global minima, both of which will impact our use of homotopy methods in Section III. Both difficulties can be ameliorated by introducing another layer of optimization: namely, for $b \in \mathbb{R}^N$ consider

$$\min\left\{ \|x-b\|_2^2 \,:\, \begin{array}{l} x \in \mathcal{V}_{\mathbb{R}}(g) \\ \|x-a\|_0 = \min\{\|y-a\|_0 \,:\, y \in \mathcal{V}(g)\} \end{array} \right\}. \tag{9}$$

In particular, this problem describes computing points $x \in \mathcal{V}_{\mathbb{R}}(g)$ nearest to b in the Euclidean norm which agree with a in the maximum number of coordinates.

Proposition II.3. *If $x^* \in \mathcal{V}_{\mathbb{R}}(g)$ solves* (9)*, then there exists $\lambda^* \in \mathbb{P}^n$ such that $G(x^*, \lambda^*) = 0$ where*

$$G(x,\lambda) = \begin{bmatrix} g(x) \\ (x-a) \circ (\lambda_0(x-b) + \sum_{i=1}^n \lambda_i \nabla g_i(x)) \end{bmatrix} \tag{10}$$

and $\circ$ denotes the Hadamard (entrywise) product.

Proof: Let $J = \{j \,:\, x_j^* = a_j\}$ and $m = \#J$. By reordering the coordinates, we can assume without loss of generality that $J = \{N-m+1, \ldots, N\}$. Let $\pi : \mathbb{R}^{N-m} \to \mathbb{R}^N$ be defined by $\pi(z) = (z, a)$. Thus, for $\alpha = (a_1, \ldots, a_{N-m})$, $z^* = (x_1^*, \ldots, x_{N-m}^*)$ solves

$$\min\{\|z-\alpha\|_2^2 \,:\, \pi(z) \in \mathcal{V}_{\mathbb{R}}(g)\}.$$

Hence, Prop. II.1 yields $\lambda^* \in \mathbb{P}^n$ such that (z^*, λ^*) solves

$$\begin{bmatrix} g(\pi(z)) \\ \lambda_0(z-\alpha) + \sum_{i=1}^n \lambda_i \nabla g_i(\pi(z)) \end{bmatrix} = 0.$$

Since $x_j^* = a_j$ for $j \in J$, the result immediately follows. ■

The system G in (10) is the *critical point system* for (8) and the set of *critical points* of (8) is the set of points x such that there exists $\lambda \in \mathbb{P}^n$ with $G(x,\lambda) = 0$. In fact, the previous proof can be extended to show that the set of critical points consists of critical points on every possible choice of slices $x_j = a_j$ for $j \in J \subset \{1, \ldots, N\}$.

Example II.4. For g and a from Ex. II.2 with $b = a$,

$$G(x,\lambda) = \begin{bmatrix} x_1^2 + x_2^2 - 1 \\ (x_1 + 0.6)(\lambda_0(x_1 + 0.6) + \lambda_1(2x_1)) \\ (x_2 - 0.45)(\lambda_0(x_2 - 0.45) + \lambda_1(2x_2)) \end{bmatrix}$$

yields 6 critical points: p_1 and p_2 from Ex. II.2 and

$$\begin{aligned} p_3 &= (-0.6, 0.8), & p_4 &= (-0.6, -0.8), \\ p_5 &= (-\sqrt{0.7975}, 0.45), & p_6 &= (\sqrt{0.7975}, 0.45). \end{aligned}$$

The points p_1 and p_2 are the global minimizer and maximizer for $J = \emptyset$, p_3 and p_4 are the global minimizer and maximizer for $J = \{1\}$, and p_5 and p_6 are the global minimizer and maximizer for $J = \{2\}$, respectively, which are shown in Figure 1. Thus, $p_3, \ldots, p_6$, are all global minimizers for (8).

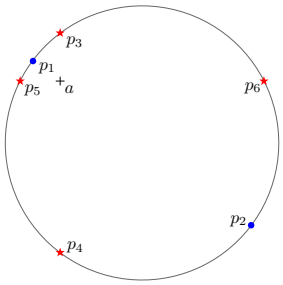

Figure 1. Hamming critical points for the unit circle from Ex. II.4. The stars are the global minimizers while the blue dots are the Euclidian distance (ℓ_2) global minimizer and maximizer from Ex. II.2.

In (8), the objective function was dependent upon all variables. A natural extension of Prop. II.3 applies if one considers only a subset of the variables. For example, if $h : \mathbb{R}^N \times \mathbb{R}^M \to \mathbb{R}^n$ is a real polynomial system and $a \in \mathbb{R}^N$, consider

$$\min\{\|x-a\|_0 : (x,y) \in \mathcal{V}_{\mathbb{R}}(h)\}.$$

For $b \in \mathbb{R}^N$ and $c \in \mathbb{R}^M$, the corresponding critical point system is

$$\begin{bmatrix} h(x,y) \\ (x-a) \circ (\lambda_0(x-b) + \sum_{i=1}^n \lambda_i \nabla_x h_i(x,y)) \\ \lambda_0(y-c) + \sum_{i=1}^n \lambda_i \nabla_y h_i(x,y) \end{bmatrix} \quad (11)$$

where $\nabla_z h_i(x,y)$ is the gradient of h_i with respect to z evaluated at (x,y).

C. Minimizing $\|x\|_1$

For $a \in \mathbb{R}^N$, we aim to derive necessary conditions for

$$\min\{\|x-a\|_1 : x \in \mathcal{V}_{\mathbb{R}}(g)\} \quad (12)$$

via a polynomial system. Although $x \mapsto \|x-a\|_1$ is continuous, it is not differentiable. However, for $x \in \mathbb{R}^N$ with $x_i \neq a_i$,

$$\frac{\partial}{\partial x_i}\|x-a\|_1 = \operatorname{sign}(x_i - a_i) = \begin{cases} 1 & \text{if } x_i > a_i \\ -1 & \text{if } x_i < a_i. \end{cases}$$

To avoid the piecewise nature, we square, yielding

$$\left(\frac{\partial}{\partial x_i}\|x-a\|_1\right)^2 = 1.$$

This leads to the following necessary conditions.

Proposition II.5. *If $x^* \in \mathcal{V}_{\mathbb{R}}(g)$ solves* (12)*, then there exists $\lambda^* \in \mathbb{P}^n$ such that $G(x^*,\lambda^*) = 0$ where*

$$G(x,\lambda) = \begin{bmatrix} g(x) \\ (x-a) \circ \left(\lambda_0^2 \mathbb{1} - (\sum_{i=1}^n \lambda_i \nabla g_i(x))^{\circ 2}\right) \end{bmatrix} \quad (13)$$

and $\circ$ denotes the Hadamard (entrywise) product, $\mathbb{1}$ denotes the vector of all ones, and $v^{\circ 2} = v \circ v$.

Proof: Let $J = \{j : x_j^* = a_j\}$ and $m = \#J$. By reordering the coordinates, we can assume without loss of generality that $J = \{N-m+1, \ldots, N\}$. Let $\pi : \mathbb{R}^{N-m} \to \mathbb{R}^N$ be defined by $\pi(z) = (z,a)$. Hence, for $\alpha = (a_1, \ldots, a_{N-m})$, $z^* = (x_1^*, \ldots, x_{N-m}^*)$ solves

$$\min\{\|z-\alpha\|_1 : \pi(z) \in \mathcal{V}_{\mathbb{R}}(g)\}.$$

Since $z \mapsto \|z-\alpha\|_1$ is differentiable at z^*, Fritz John conditions yield $\lambda^* \in \mathbb{P}^n$ where (z^*,λ^*) satisfies

$$\lambda_0 \frac{\partial}{\partial z_j}\|z-\alpha\|_1 + \sum_{i=1}^n \lambda_i \frac{\partial}{\partial z_j} g(\pi(z)) = 0$$

for $j = 1, \ldots, N-m$. Hence, (z^*,λ^*) satisfies

$$\lambda_0^2 = \left(\lambda_0 \frac{\partial}{\partial z_j}\|z-\alpha\|_1\right)^2 = \left(\sum_{i=1}^n \lambda_i \frac{\partial}{\partial z_j} g(\pi(z))\right)^2$$

for $j = 1, \ldots, N-m$. This shows that (x^*,λ^*) solves the first $N-m$ equations of

$$(x-a) \circ \left(\lambda_0^2 \mathbb{1} - \left(\sum_{i=1}^n \lambda_i \nabla g_i(x)\right)^{\circ 2}\right) = 0.$$

The last m equations are satisfied since $x_j^* = a_j$ for $j \in J$. ∎

The system G in (13) is the *critical point system* for (12) and the set of *critical points* of (12) is the set of points x such that there exists $\lambda \in \mathbb{P}^n$ with $G(x,\lambda) = 0$. Due to the squaring, if $\lambda = [\lambda_0, \ldots, \lambda_n]$ with $G(x,\lambda) = 0$, then $G(x,\lambda') = 0$ where $\lambda' = [-\lambda_0, \lambda_1, \ldots, \lambda_n]$. Therefore, a necessary condition for a real critical point x to solve (12) is to have $\lambda \in \mathbb{P}^n$ satisfy

$$\operatorname{sign}(\lambda_0(a_j - x_j)) = \operatorname{sign}\left(\sum_{i=1}^n \lambda_i \nabla g_i(x_j)\right) \quad (14)$$

for all j with $x_j \neq a_j$. This is trivially satisfied if $\lambda_0 = 0$.

Example II.6. For g and a from Ex. II.2,

$$G(x,\lambda) = \begin{bmatrix} x_1^2 + x_2^2 - 1 \\ (x_1 + 0.6)(\lambda_0^2 - (2x_1\lambda_1)^2) \\ (x_2 - 0.45)(\lambda_0^2 - (2x_2\lambda_1)^2) \end{bmatrix}$$

yields 16 solutions which map 2-to-1 to the following set of 8 critical points: $p_3, \ldots, p_6$ from Ex. II.4, together with

$$p_7 = (\sqrt{1/2}, \sqrt{1/2}), \quad p_8 = (-\sqrt{1/2}, \sqrt{1/2}),$$
$$p_9 = (\sqrt{1/2}, -\sqrt{1/2}), \quad p_{10} = (-\sqrt{1/2}, -\sqrt{1/2}).$$

Each of the four points $p_3, \ldots, p_6$ are local minimizers with p_5 being the global minimizer for (12). Each of the four points $p_7, \ldots, p_{10}$ are local maximizers with p_9 being

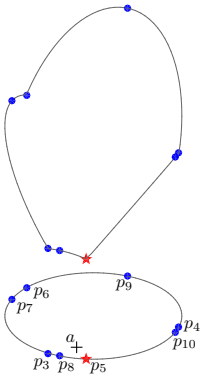

Figure 2. Taxicab critical points and the objective function over the unit circle. The star is the global minimizer and the blue dots are other critical points for Ex. II.6.

the global maximizer. Figure 2 shows the critical points and the value of the objective function on the unit circle.

Example II.7. Repeating Ex. II.2, II.4, and II.6 with $a = (-0.6, 0.95)$ yields the following global minimizers (with numerical approximations listed to 4 decimal places):

ℓ_2 : $(-0.5340, 0.8455)$
ℓ_0 : $(-0.6, \pm 0.8)$, $(\pm 0.3122, 0.95)$
ℓ_1 : $(-0.6, 0.8)$.

We note that $p_7, \ldots, p_{10}$ from Ex. II.6 were ℓ_1 critical points, with only p_9 and p_{10} satisfying the sign condition (14).

One advantage of defining the critical point set without enforcing reality or (14) is that the critical point set is an algebraic set, i.e., closed in the Zariski topology on $\mathbb{C}^N$. This is exemplified in the following.

Example II.8. For $g(x) = x_1^2 + x_2^2 - 1$ and $a = (0, 0)$, every point satisfying $g = 0$ is a critical point of (6) where the set of global minimizers is $\mathcal{V}_{\mathbb{R}}(g)$. For $g(x) = x_1 + x_2 - 1$ and *any* $a \in \mathbb{R}^2$, every point satisfying $g = 0$ is a critical point of (12) where the set of global minimizers is the line segment $t(a_1, 1 - a_1) + (1 - t)(1 - a_2, a_2)$ for $t \in [0, 1]$.

III. Critical point homotopies

Since the set of critical points need not be finite, this section extends the construction of a critical point homotopy for (6) developed in [12] to compute a finite subset of the critical points containing a global minimizer under certain assumptions. For the real polynomial system $g : \mathbb{R}^N \to \mathbb{R}^n$, we assume:

($\mathcal{A}$) each irreducible component of $\mathcal{V}_{\mathbb{C}}(g)$ has dimension $N - n$, i.e., codimension n.

One way to always satisfy ($\mathcal{A}$) is by replacing the polynomial system g with the polynomial $g' = \sum_{i=1}^n g_i^2$ so that $\mathcal{V}_{\mathbb{R}}(g) = \mathcal{V}_{\mathbb{R}}(g')$ and every irreducible component of $\mathcal{V}_{\mathbb{C}}(g')$ has dimension $N - 1$, i.e., codimension 1.

Throughout the remainder of the paper, a point is generic if it is outside of a Zariski closed proper subset. A non-generic point may also be called special. We refer the reader to [16], [17] for further information.

A. Homotopy for $\|x\|_2$

Given $a \in \mathbb{R}^N$ and g satisfying ($\mathcal{A}$), there are two considerations for computing a finite subset of critical points to (6): singular points of $\mathcal{V}_{\mathbb{C}}(g)$ and nongenericity of a. Since each singular point of $\mathcal{V}_{\mathbb{C}}(g)$ is trivially a critical point, systems with infinitely many singular points pose a challenge for computing a finite subset of critical points. This is addressed in [11], [12] by considering a family of perturbations of g via infinitesimals and parameter homotopies, respectively. In particular, we will assume that $\epsilon \in \mathbb{R}^N$ and $\gamma \in \mathbb{C}$ are chosen so that $\mathcal{V}_{\mathbb{C}}(g - t\gamma\epsilon)$ is smooth of codimension n for all $t \in (0, 1]$.

For special choices of a, one could have infinitely many global minimizers for (6), e.g., in Ex. II.8, the origin is the center of the unit circle. Following [11], [12], we will assume genericity of a in that one obtains the maximum number of isolated solutions for (7) applied to $g - t\gamma\epsilon$ for all $t \in (0, 1]$. The previous two assumptions hold with probability one for random choices of $\epsilon \in \mathbb{R}^N$, $\gamma \in \mathbb{C}$, and $a \in \mathbb{R}^N$ yielding the following derived from [12, Thm. 5].

Proposition III.1. *Suppose that g satisfies ($\mathcal{A}$) and $\epsilon \in \mathbb{R}^N$, $\gamma \in \mathbb{C}$, and $a \in \mathbb{R}^N$ satisfy the aforementioned genericity assumptions. Then, the homotopy*

$$H(x, \lambda, t) = \begin{bmatrix} g(x) - t\gamma\epsilon \\ \lambda_0(x - a) + \sum_{i=1}^n \lambda_i \nabla g_i(x) \end{bmatrix} = 0$$

defines finitely many smooth solution paths for $t \in (0, 1]$ and the set of x-coordinates for the finite endpoints at $t = 0$ is a finite set of critical points containing a global minimizer of (6).

Remark III.2. This immediately provides a three-step process for solving (6): solve $H(x, \lambda, 1) = 0$ to compute the start points, compute the x-coordinates of the endpoints at $t = 0$ defined by $H(x, \lambda, t) = 0$, and sort through the endpoints to find a global minimizer. One approach to computing the start points is to utilize regeneration [19], and exploit the 2-homogeneous structure [20]. More details regarding using numerical algebraic geometry to solve $H(x, \lambda, 1) = 0$ and track the paths defined by $H(x, \lambda, t) = 0$ can be found in the books [17], [21].

Example III.3. Consider the polynomial system

$$g(x) = \begin{bmatrix} x_1^2 - x_2 \\ x_1 x_2 - x_3 \\ x_1 x_3 - x_2^2 \end{bmatrix} = 0$$

which defines the twisted cubic curve. Hence, g consists of 3 polynomials while $\mathcal{V}_{\mathbb{C}}(g)$ has codimension 2. We consider two ways to satisfy $(\mathcal{A})$:

- selecting a well-constrained subset, namely

$$G_1(x) = \begin{bmatrix} x_1^2 - x_2 \\ x_1x_2 - x_3 \end{bmatrix};$$

- taking a sum of squares, namely

$$G_2(x) = (x_1^2 - x_2)^2 + (x_1x_2 - x_3)^2 + (x_1x_3 - x_2^2)^2.$$

For $a = (2, 4, 2)$, applying Prop. III.1 with either G_1 or G_2 yields a unique real critical point, namely $t_1 = (1.4395, 2.0722, 2.9830)$ which is listed to 4 decimal places and shown as the blue dot in Figure 3. For G_1, 5 paths are tracked with one converging to t_1. For G_2, 32 paths are tracked with two converging to t_1.

B. Homotopy for $\|x\|_0$

The free choice of $b \in \mathbb{R}^N$ in (9) and (10) removes any genericity assumption on a in this case. However, the genericity assumption on ϵ and γ are slightly increased in that one now requires the smoothness of

$$\bigcup_{J\subset\{1,\ldots,n\}} \mathcal{V}_{\mathbb{C}}(g(x) - t\gamma\epsilon) \cap \mathcal{V}_{\mathbb{C}}(x_j - a_j, j \in J) \qquad (15)$$

for all $t \in (0, 1]$, which is still satisfied with probability one.

Proposition III.4. *Suppose that g satisfies $(\mathcal{A})$ and each of $\epsilon \in \mathbb{R}^N$, $\gamma \in \mathbb{C}$, and $b \in \mathbb{R}^N$ satisfy the genericity assumptions as in Prop. III.1. Then the homotopy*

$$H(x, \lambda, t) = \begin{bmatrix} g(x) - t\gamma\epsilon \\ (x - a) \circ \left(\lambda_0(x - b) + \sum_{i=1}^n \lambda_i \nabla g_i(x)\right) \end{bmatrix} = 0$$

defines finitely many smooth solutions paths for $t \in (0, 1]$ and the set of x-coordinates for the finite endpoints at $t = 0$ is a finite set of critical points containing a global minimizer of (8).

Proof: It immediately follows from Prop. III.1 that this computes a global minimizer of

$$\min\{\|x - b\|_2^2 : x \in \mathcal{V}_{\mathbb{R}}(g),\ x_j = a_j \text{ for } j \in J\}$$

for each choice of $J \subset \{1, \ldots, n\}$. Hence, one obtains a global minimizer of (8). ∎

One has a similar three-step solving procedure for solving (8) as in Remark III.2.

Example III.5. With the setup from Ex. III.3, applying Prop. III.4 to either G_1 or G_2 yields 4 real critical points, namely t_1 from Ex. III.3 and, to 4 decimal places:

$$t_2 = (1.2599, 1.5874, 2),\ \ t_3 = (-2, 4, -8),\ \ t_4 = (2, 4, 8).$$

The point t_4 is the global minimizer of (8) which is shown in Figure 3. For G_1, 11 paths are tracked with 5 converging to real points: one each to t_1, t_2, t_3 and two to t_4. For G_2, 80 paths are tracked with 12 converging to real points: two each to t_1, t_2, t_3 and six to t_4.

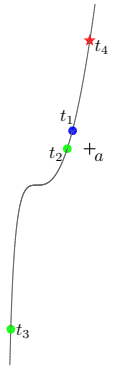

Figure 3. Hamming critical points for the twisted cubic. The red star is the global ℓ_0 minimizer with two coordinates equal. The green dots are critical points with one coordinate equal. The blue dot, which has no coordinates equal, is the global ℓ_2 minimizer from Ex. III.3.

C. Homotopy for $\|x\|_1$

In contrast to (6), for which only special values of a yield infinitely many global minimizers, Ex. II.8 shows that this need not be the case for (12). Thus, we will additionally assume that there is an isolated point in the set of global minimizers to (12). A genericity assumption on ϵ and γ yielding smoothness in (15) for $t \in (0, 1]$ yields the following.

Proposition III.6. *Suppose that g satisfies $(\mathcal{A})$ and $\epsilon \in \mathbb{R}^N$, $\gamma \in \mathbb{C}$, and $a \in \mathbb{R}^N$ satisfy the aforementioned genericity assumptions and those in Prop. III.1. Then, the homotopy*

$$H(x, \lambda, t) = \begin{bmatrix} g(x) - t\gamma\epsilon \\ (x - a) \circ \left(\lambda_0^2\mathbb{1} - \left(\sum_{i=1}^n \lambda_i \nabla g_i(x)\right)^{\circ 2}\right) \end{bmatrix} = 0$$

defines finitely many smooth solution paths for $t \in (0, 1]$ and the set of x-coordinates for the finite endpoints at $t = 0$ is a finite set of critical points containing a global minimizer of (12).

Proof: The genericity assumptions yield smooth solution paths for $t \in (0, 1]$. Thus, it only remains to show that one obtains a critical point that is a global minimizer of (12). This follows from the assumption regarding the existence of an isolated global minimizer together with the theory of parameter homotopies [22] extended in [23]. ∎

Again, one has a similar three-step solving procedure for solving (12) as in Remark III.2.

Example III.7. With the setup from Ex. III.3, applying Prop. III.6 to either G_1 or G_2 yields 7 real critical points, namely t_2, t_3, t_4 from Ex. III.5 along with

$$t_5 = (1, 1, 1), \qquad t_6 = (1/3, 1/9, 1/27),$$
$$t_7 = (-1/3, 1/9, -1/27), \quad t_8 = (-1, 1, -1).$$

The global minimizer of (12) is t_2, which is shown in Figure 4. For G_1, 40 paths are tracked with 24 converging

to real points: four each to t_2 and t_3, eight to t_4, and two each to $t_5, \ldots, t_8$. Moreover, the points $t_5, \ldots, t_8$ fail the sign condition (14). For G_2, 292 paths are tracked with 52 converging to real points: eight each to t_2 and t_3, twenty to t_4, and four each to $t_5, \ldots, t_8$. All critical points trivially satisfy the sign condition (14) due to $\lambda_0 = 0$.

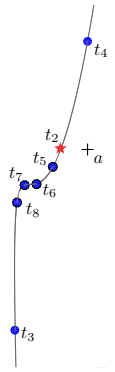

Figure 4. Taxicab critical points for the twisted cubic. The red star is the global ℓ_1 minimizer. Critical points $t_5, \ldots t_8$ fail the sign condition (14) with respect to G_1 and trivially pass with respect to G_2.

IV. Local homotopies

The homotopies in Prop. III.1, III.4, and III.6 are global homotopies in that all paths are smooth for $t \in (0, 1]$ and one obtains a global minimizer under proper assumptions. In this section, we turn to local homotopies derived from [24] that aim to locate a critical point near a given real point. With these local homotopies, there is no guarantee that the path will be smooth for $t \in (0, 1]$. However, if it is smooth, the endpoint corresponds with a real critical point.

A. Local homotopy for $\|x\|_2$

As described in [24], given a real polynomial system $g : \mathbb{R}^N \to \mathbb{R}^n$ and $x^* \in \mathbb{R}^N$, one considers the homotopy

$$H(x, \lambda, t) = \begin{bmatrix} g(x) - tg(x^*) \\ \lambda_0(x - x^*) + \sum_{i=1}^n \lambda_i \nabla g_i(x) \end{bmatrix} = 0 \tag{16}$$

with start point, at $t = 1$, $x = x^*$ and $\lambda = [1, 0, \ldots, 0]$. This is called a *gradient descent homotopy* in [24].

B. Local homotopy for $\|x\|_0$

If one knows *a priori* which coordinates of x^* should remain fixed, i.e., knows $J \subset \{1, \ldots, n\}$ such that one aims to locate a point on $\mathcal{V}_{\mathbb{R}}(g) \cap \mathcal{V}_{\mathbb{R}}(x_j - x_j^*, j \in J)$, then one can simply modify the gradient descent homotopy (16) appropriately. This would aim to locate a point closest to the given point x^* in the ℓ_2-norm which has the same set of J coordinates at x^*.

Since this information is often not known, we consider an alternative approach. Suppose that one is given $a, x^* \in \mathbb{R}^N$ such that $a_i \neq x_i^*$ for $i = 1, \ldots, N$. Then, one could try the homotopy $H(x, \lambda, t)$ given by

$$\begin{bmatrix} g(x) - tg(x^*) \\ (x - a) \circ \big(\lambda_0(x - a) + \sum_{i=1}^n \lambda_i \nabla g_i(x)\big) - t\lambda_0(x^* - a)^{\circ 2} \end{bmatrix} \tag{17}$$

with start point, at $t = 1$, $x = x^*$ and $\lambda = [1, 0, \ldots, 0]$.

C. Local homotopy for $\|x\|_1$

Rather than utilize squaring as in Prop. III.6, we consider the following local homotopy $H(x, \lambda, t)$ given $a, v, x^* \in \mathbb{R}^N$ such that $a_i \neq x_i^*$ for $i = 1, \ldots, N$:

$$\begin{bmatrix} g(x) - tg(x^*) \\ (x - a) \circ (\lambda_0 v + \sum_{i=1}^n \lambda_i \nabla g_i(x)) - t\lambda_0(x^* - a) \circ v \end{bmatrix} \tag{18}$$

with start point, at $t = 1$, $x = x^*$ and $\lambda = [1, 0, \ldots, 0]$. In the special case that $v^{\circ 2} = \mathbb{1}$ and the path is smooth for $t \in (0, 1]$, then the endpoint corresponds to a real critical point for (12).

D. Local homotopy example

The local homotopy (16) was applied to 500 points uniformly sampled in $[-3, 3]^2$ for

$$g(x) = x_2^2 + x_1^2(x_1 - 1)(x_1 - 2)$$

in [24, Fig. 3(a)]. With $a = 0$, Figure 5 shows the same setup for the local homotopy (17).

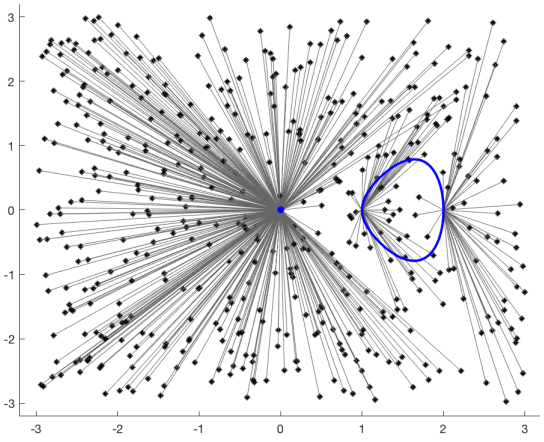

Figure 5. Results of local homotopy (17) with $\mathcal{V}_{\mathbb{R}}(g)$ shown in blue.

We also applied the local homotopy (18) with $a = 0$ and

$$v = \frac{\nabla g(x^*)}{\|\nabla g(x^*)\|_2}.$$

The results are shown in Figure 6.

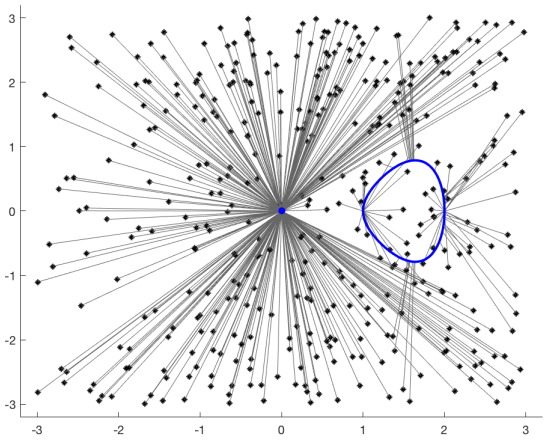

Figure 6. Results of local homotopy (18) with $\mathcal{V}_{\mathbb{R}}(g)$ shown in blue.

V. Additional Examples

A. Torus

Consider the torus with $R = 2$ and $r = 0.5$ defined by

$$g = (x^2 + y^2 + z^2 + R^2 - r^2)^2 - 4R^2(x^2 + y^2) = 0.$$

For $a = (0.45, 1, 0.2)$, applying Prop. III.4 yields 24 distinct real critical points for the Hamming distance which are plotted in Figure 7. In particular, there are 8 global minimizers which are (to 4 decimal places):

$$\begin{aligned} q_1 &= (0.45, 1.4746, 0.2), & q_2 &= (0.45, 2.4167, 0.2), \\ q_3 &= (2.2457, 1, 0.2), & q_4 &= (1.1734, 1, 0.2), \\ q_5 &= (-1.1734, 1, 0.2), & q_6 &= (-2.2457, 1, 0.2), \\ q_7 &= (0.45, -1.4746, 0.2), & q_8 &= (0.45, -2.4167, 0.2). \end{aligned}$$

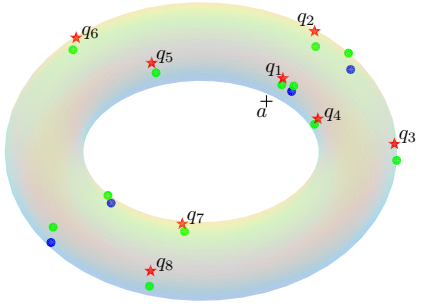

Figure 7. Hamming critical points on the torus. The stars are the global minimizers with two coordinates being equal. The other colored dots are critical points having either one (green) or no (blue) coordinates equal.

Next, applying Prop. III.6 yields 48 distinct real critical points for the taxicab distance which are plotted in Figure 8. Of these, 32 satisfy the sign condition (14) with the global minimizer being q_1.

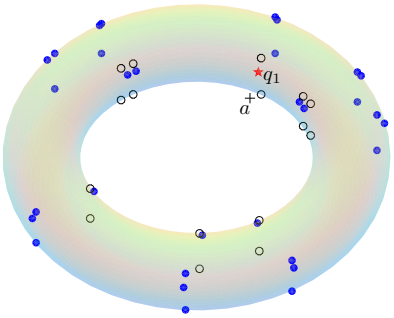

Figure 8. Taxicab critical points on the torus. The star is the global minimizer. The blue dots are other critical points which satisfy the sign condition (14) while the black circles fail this condition.

B. Matrix Rigidity

We close by recovering a low rank matrix from a given matrix which has possibly undergone transcription errors. In particular, we aim to compute the *r-rigidity* [25], [26], [27] of an $n \times n$ matrix M, which equals

$$\min\{\|E\|_0 \ : \ M = A + E, \ \ \text{rank } A \leq r\}.$$

Specifically, we demonstrate our homotopy-based approach for computing the 1-rigidity of selected matrices in $\mathbb{R}^{3\times 3}$. Since rank $A \leq 1$, we write $A = uv^T$, u and $v \in \mathbb{R}^3$, and assume $v_1 = 1$. Thus, we can utilize the polynomial system (11) to enforce the sparsity condition on E as well as taking the vector of coordinates (E, u, v) to be as close to the origin (with respect to the 2-norm) as possible. For generic M, this system yields 1593 critical points.

Deforming from a generic M to the rank 2 matrix

$$M' = \begin{bmatrix} 1 & 1 & 1 \\ 2 & 0 & 0 \\ 3 & 0 & 0 \end{bmatrix}$$

yields 405 paths that converge to real points with 225 distinct values for (E, u, v). The two Hamming minimizers

$$u = \begin{bmatrix} 1 \\ 0 \\ 0 \end{bmatrix}, \quad v = \begin{bmatrix} 1 \\ 1 \\ 1 \end{bmatrix}, \quad E = \begin{bmatrix} 0 & 0 & 0 \\ 2 & 0 & 0 \\ 3 & 0 & 0 \end{bmatrix}$$

and

$$u = \begin{bmatrix} 1 \\ 2 \\ 3 \end{bmatrix}, \quad v = \begin{bmatrix} 1 \\ 0 \\ 0 \end{bmatrix}, \quad E = \begin{bmatrix} 0 & 1 & 1 \\ 0 & 0 & 0 \\ 0 & 0 & 0 \end{bmatrix}$$

have 4 paths converging to each of them. Hence, the 1-rigidity of M' is 2.

Finally, we consider the full rank matrix

$$M'' = \begin{bmatrix} 2 & 2 & 3 \\ -3 & 2 & -6 \\ -2 & 1 & -3 \end{bmatrix}.$$

For this matrix, 423 paths converged to real points with 346 distinct values for (E, u, v). The unique Hamming minimizer, which was the endpoint of 15 paths, is

$$u = \begin{bmatrix} 2 \\ -4 \\ -2 \end{bmatrix}, \quad v = \begin{bmatrix} 1 \\ -1/2 \\ 3/2 \end{bmatrix}, \quad E = \begin{bmatrix} 0 & 3 & 0 \\ 1 & 0 & 0 \\ 0 & 0 & 0 \end{bmatrix}.$$

Hence, the 1-rigidity of M'' is also 2.

ACKNOWLEDGMENT

JDH and SNS were partially supported by NSF CCF 1812746 and ONR N00014-16-1-2722. SNS was also partially supported by Schmitt Leadership Fellowship in Science and Engineering.

REFERENCES

[1] R. Hamming, "Error detecting and error correcting codes," *Bell System Technical Journal*, vol. 29, no. 2, pp. 147–160, 1950.

[2] E. Candes, J. Romberg, and T. Tao, *Communications on Pure and Applied Mathematics*, vol. 59, no. 8, pp. 1207–1223, 2006.

[3] D. Donoho, "Compressed sensing," *IEEE Transactions on Information Theory*, vol. 52, no. 4, pp. 1289–1306, 2006.

[4] E. Candes, M. Rudelson, T. Tao, and R. Vershynin, "Error correction via linear programming," in *46th Annual IEEE Symposium on Foundations of Computer Science, 2005. FOCS 2005.* IEEE, 2005, pp. 668–681.

[5] A. Yang, S. Sastry, A. Ganesh, and Y. Ma, "Fast ℓ_1-minimization algorithms and an application in robust face recognition: A review," in *2010 17th IEEE International Conference on Image Processing (ICIP)*. IEEE, 2010, pp. 1849–1852.

[6] M. Lustig, D. Donoho, and J. Pauly, "Sparse MRI: The application of compressed sensing for rapid MR imaging," *Magnetic Resonance in Medicine*, vol. 58, no. 6, pp. 1182–1195, 2007.

[7] G. Davis, S. Mallat, and M. Avellaneda, "Adaptive greedy approximations," *Constructive Approximation*, vol. 13, no. 1, pp. 57–98, 1997.

[8] S. Chen, D. Donoho, and M. Saunders, "Atomic decomposition by basis pursuit," *SIAM Journal on Scientific Computing*, vol. 20, no. 1, pp. 33–61, 1998.

[9] H. Ohlsson, A. Yang, R. Dong, and S. Sastry, "Nonlinear basis pursuit," in *2013 Asilomar Conference on Signals, Systems and Computers*, Nov 2013, pp. 115–119.

[10] A. Seidenberg, "A new decision method for elementary algebra," *Annals of Mathematics*, vol. 60, no. 2, pp. 365–374, 1954.

[11] F. Rouillier, M.-F. Roy, and M. Safey El Din, "Finding at least one point in each connected component of a real algebraic set defined by a single equation," *J. Complexity*, vol. 16, no. 4, pp. 716–750, 2000.

[12] J. Hauenstein, "Numerically computing real points on algebraic sets," *Acta Applicandae Mathematicae*, vol. 125, no. 1, pp. 105–119, 2013.

[13] J. Draisma, E. Horobeţ, G. Ottaviani, B. Sturmfels, and R. Thomas, "The Euclidean distance degree," in *SNC 2014—Proceedings of the 2014 Symposium on Symbolic-Numeric Computation*. ACM, New York, 2014, pp. 9–16.

[14] ——, "The Euclidean distance degree of an algebraic variety," *Found. Comput. Math.*, vol. 16, no. 1, pp. 99–149, 2016.

[15] E. Gross, B. Davis, K. Ho, D. Bates, and H. Harrington, "Numerical algebraic geometry for model selection and its application to the life sciences," *Journal of The Royal Society Interface*, vol. 13, no. 123, p. 20160256, 2016.

[16] D. Cox, J. Little, and D. O'Shea, *Ideals, Varieties, and Algorithms: An Introduction to Computational Algebraic Geometry and Commutative Algebra*, 4th ed. Springer Publishing Company, Incorporated, 2015.

[17] A. Sommese and C. Wampler, *The Numerical Solution of Systems of Polynomials Arising in Engineering and Science*. World Scientific, 2005, vol. 99.

[18] F. John, "Extremum problems with inequalities as subsidiary conditions," in *Studies and Essays Presented to R. Courant on his 60th Birthday, January 8, 1948*. Interscience Publishers, Inc., New York, N. Y., 1948, pp. 187–204.

[19] J. Hauenstein, A. Sommese, and C. Wampler, "Regeneration homotopies for solving systems of polynomials," *Mathematics of Computation*, vol. 80, no. 273, pp. 345–377, 2011.

[20] J. Hauenstein and J. Rodriguez, "Multiprojective witness sets and a trace test," To appear in *Adv. Geom.*

[21] D. Bates, J. Hauenstein, A. Sommese, and C. Wampler, *Numerically Solving Polynomial Systems with Bertini*. SIAM, 2013, vol. 25.

[22] A. Morgan and A. Sommese, "Coefficient-parameter polynomial continuation," *Appl. Math. Comput.*, vol. 29, no. 2, part II, pp. 123–160, 1989.

[23] D. Bates, D. Brake, J. Hauenstein, A. Sommese, and C. Wampler, "Homotopies for connected components of algebraic sets with application to computing critical sets," in *Mathematical Aspects of Computer and Information Sciences*. Cham: Springer International Publishing, 2017, pp. 107–120.

[24] Z. Griffin and J. Hauenstein, "Real solutions to systems of polynomial equations and parameter continuation," *Adv. Geom.*, vol. 15, no. 2, pp. 173–187, 2015.

[25] L. Valiant, "Graph-theoretic arguments in low-level complexity," pp. 162–176. Lecture Notes in Comput. Sci., Vol. 53, 1977.

[26] A. Kumar, S. Lokam, V. Patankar, and M. Sarma, "Using elimination theory to construct rigid matrices," *Comput. Complexity*, vol. 23, no. 4, pp. 531–563, 2014.

[27] F. Gesmundo, J. Hauenstein, C. Ikenmeyer, and J. Landsberg, "Complexity of linear circuits and geometry," *Found. Comput. Math.*, vol. 16, no. 3, pp. 599–635, 2016.